FULL PAPER

Open Access

CrossMark

Competition between winds and electric fields in the formation of blanketing sporadic E layers at equatorial regions

Laysa Cristina Araújo Resende[1*] , Inez Staciarini Batista[1], Clezio Marcos Denardini[1], Alexander José Carrasco[2], Vânia de Fátima Andrioli[1,3], Juliano Moro[3,4], Paulo Prado Batista[1] and Sony Su Chen[1]

Abstract

In the present work, we analyze the competition between tidal winds and electric fields in the formation of blanketing sporadic E layers (Es_b) over São Luís, Brazil (2° 31′ S, 44° 16′ W), a quasi-equatorial station. To investigate this competition, we have used an ionospheric E region model (MIRE) that is able to model the Es_b layers taking into account the E region winds and electric fields. The model calculates the densities for the main molecular and metallic ions by solving the continuity and momentum equations for each of the species. Thus, the main purpose of this analysis is to verify the electric fields role in the occurrence or disruption of Es_b layers through simulations. The first results of the simulations show that the Es_b layer is usually present when only the tidal winds were considered. In addition, when the zonal component of the electric field is introduced in the simulation, the Es_b layers do not show significant changes. However, the simulations show the disruption of the Es_b layers when the vertical electric field is included. In this study, we present two specific cases in which Es_b layers appear during some hours over São Luís. We can see that these layers appear when the vertical electric field was weak, which means that the tidal components were more effective during these hours. Therefore, the vertical component of the electric field is the main agent responsible for the Es_b layer disruption.

Keywords: Sporadic E layer, Tidal winds, Electric field, E region model

Introduction

The ionospheric E region frequently shows patches of enhanced electron density, known as sporadic E layers (Es). These layers are observed from 90 to 130 km, and they have a large variability that depends on the altitude and latitude. The Es layers are constituted of metallic ions (like Mg^+, Si^+, Fe^+, Ca^+, Na^+), and they have different formation mechanism according to the region of the globe where they are detected, i.e., equatorial, middle/low latitude, and auroral (Whitehead 1961; Layzer 1972; Kopp 1997; Mathews 1998; Haldoupis 2011).

The Es layers formation, at low and middle latitudes, depends essentially on the vertical wind shear associated with the tidal winds. In this process, the metallic ions are strongly Lorentz-forced to move vertically and they can be converged in a thin layer due to meridional or zonal wind components in opposite directions (Axford 1963; Chimonas and Axford 1968). Since the plasma must remain neutral, the electrons follow the magnetic field lines, which, in turn, allow that a new layer can be created (Haldoupis et al. 2007). Generally, these winds are driven by diurnal, semidiurnal and terdiurnal tides present in the E region (Mathews 1998; Wilkinson et al. 1992; Haldoupis 2011; Oikonomou et al. 2014; Pignalberi et al. 2014). These sporadic E layers are classified as blanketing layers (Es_b) (see, for example, Piggot and Rawer 1972) due to their capacity of (partially or totally) blocking the reflection of radio waves from the upper layers. These layers are formed by winds at latitudes away from the magnetic equator and have a major occurrence during the summer due to larger metallic particles entrance

*Correspondence: laysa.resende@gmail.com; laysa@dae.inpe.br
[1] National Institute for Space Research (INPE), São José dos Campos, SP, Brazil
Full list of author information is available at the end of the article

Resende *et al. Earth, Planets and Space* (2016) 68:201

Page 2 of 14

in the atmosphere during this period (Haldoupis et al. 2007).

A diffuse and non-blanketing Es trace commonly observed on daytime ionograms as a scattering of the radio signal that covers most of the frequency scale in the vicinity of the magnetic dip equator is known as q-type Es, or Es_q (Knecht and Mcduffie 1962). The Es_q traces on ionograms are associated with the Equatorial Electrojet Current (EEJ) plasma instabilities (Forbes 1981), mainly the gradient drift instability (Type II irregularities) driven by the vertical polarization electric field produced by a Hall current as well as by the vertical density gradient (Chandra and Rastogi 1975; Reddy and Devasia 1973).

The occurrence of Es_b layers over the equatorial region was reported by many authors. Rastogi (1971) and Fambitakoye et al. (1973) show that they occur during Counter Electrojet (CEJ) events that are periods during which the natural current of the EEJ is reversed, and the Es_q trace disappears. Tsunoda (2008) analyzed the Es_b layers in equatorial regions, and they suggested that these layers are anti-correlated with the EEJ intensity, in which the horizontal winds with an expressive north–south component can be responsible for their formations. At the dip equator, the Es_b layers are subject to the influence of the polarization electric field (E_p) and remain during a certain period in this sector. However, this theory needs to be investigated with more details, in order to establish the connection between E_p and Es_b occurrence. Recently, Yadav et al. (2014) studied the Es_b layer occurrence in equatorial regions in the Indian sector for the years 2007 and 2009, and they also concluded that the Es_b layers are linked with the CEJ events. In the Brazilian sector, the geomagnetic field configuration has a peculiar behavior in such a way that the magnetic inclination, at a fixed location over the northeast coast, varies at a rate of 20′ per year, corresponding to an apparent northwestward movement of the magnetic equator (Batista et al. 2011). This peculiarity of the magnetic field allowed the study of the competition between different mechanisms in the sporadic E layer formation (Abdu et al. 1996). In fact, Abdu et al. (1996) observed that other types of Es traces besides the Es_q became more frequently observed as the magnetic equator departs from Fortaleza, Brazil (3.8° S, 38° W). This fact was attributed to the reduction in the electric field influence, and the increasing predominance of other mechanisms such as wind shear. A similar study was made by Resende et al. (2013) over São Luís during magnetic storms that occurred during the solar cycle 23. They observed different types of Es_b layers that were mainly associated with the displacement of the magnetic equator in relation to the observation site. Therefore, in the Brazilian equatorial sector both Es_b and Es_q traces can occur in ionograms, offering a good opportunity to study the competition between the wind and electric field mechanisms. Thus, our discussion will focus on some interesting characteristics about the influences of winds and electric fields components using a theoretical model in order to estimate the competition of these two mechanisms in Es layers formation.
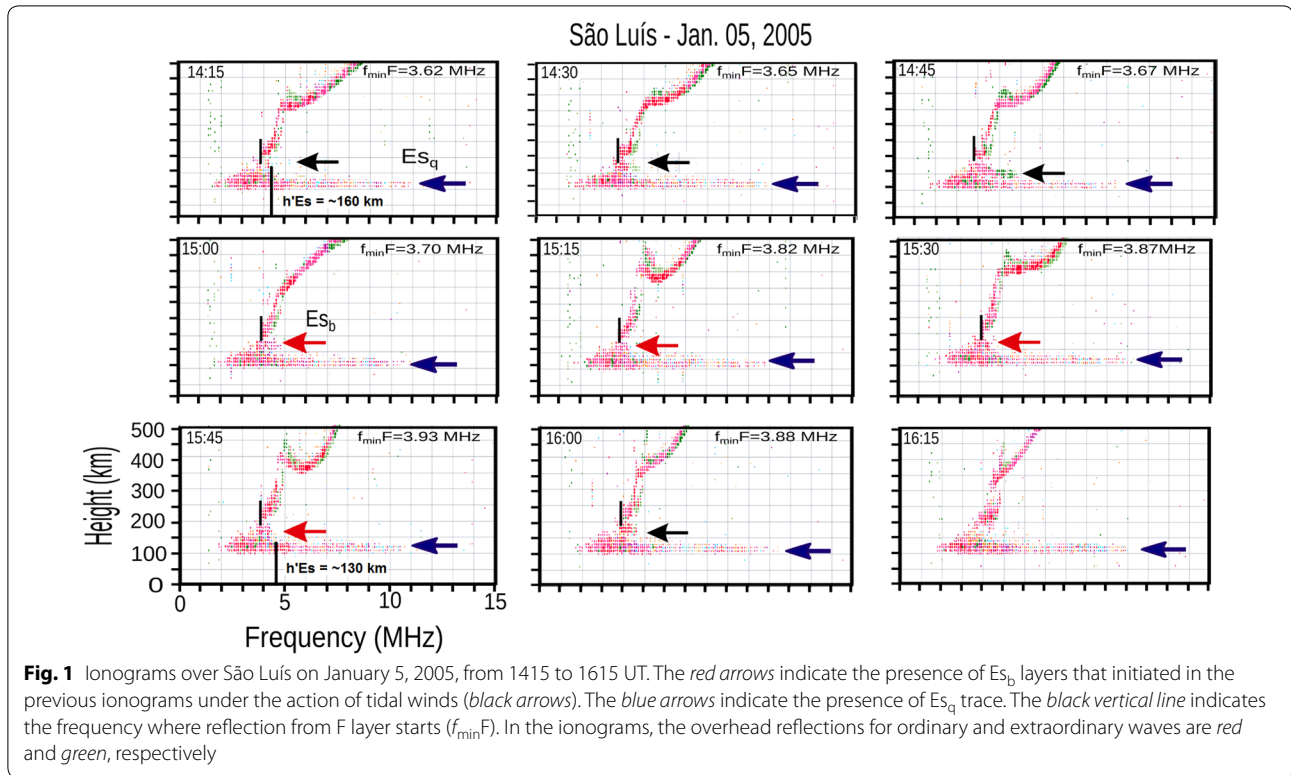
Two Es case studies

The purpose of this work is to analyze the electric fields role in the occurrence or disruption of Es_b layers through simulations. In this sense, we have selected two specific cases, January 05, 2005 and December 13, 2009, in the Brazilian quasi-equatorial site, São Luís which illustrates the process that is going to be simulated. São Luís is an interesting site for this study because it is considered a transition region in terms of EEJ current influence as can be seen in Table 1, which shows the dip angles from the year 2000 to 2015. According to Forbes (1981), a region is generally considered an Equatorial region if the magnetic inclination (dip angle) is up to 7 degrees. Thus, we can state that in 2005 São Luís could clearly be considered an equatorial site, whereas in 2009 it is almost in the limit between equatorial and non-equatorial site. In fact, we have selected the data collected during these two years when it is possible to simulate the competition process of the Es layer formation in terms of EEJ current influence.

For the first selected case, January 5, 2005, the influence of the EEJ was strong and we named it event S (Stronger EEJ event). In this case, the dip angle is -3.8 degrees (see Table 1). It can be considered a moderate disturbed day ($\sum Kp = 25, Dst > -35$ nT). In order to exemplify the appearance of the Es_b layers, a sequence of ionograms for this day, from 1415 to 1615 UT, is shown in Fig. 1 (please note that for São Luís location LT = UT-3 h). In each ionogram, the scales range from 0 to 500 km in altitude and from 0 to 15 MHz in frequency. In all the six ionograms, the Es_q trace is clearly seen and identified by a blue arrow. This was already expected because we selected an event S. Besides the Es_q, we can identify another Es trace at 1415 UT (identified by a black arrow) that persists until 1600 UT. This layer becomes stronger in each ionogram, as can be seen by its effect on partially blocking the reflection from the low-frequency end of F region above. This is indicated in the ionograms by a black vertical line and the corresponding minimum

Table 1 Dip angles for years 2000 to 2015 over São Luís

Year	Dip angle (degree)
2000	−1.9
2005	−3.8
2010	−5.7
2015	−7.8

Resende *et al. Earth, Planets and Space* (2016) 68:201

Page 3 of 14

Fig. 1 Ionograms over São Luís on January 5, 2005, from 1415 to 1615 UT. The *red arrows* indicate the presence of Es$_b$ layers that initiated in the previous ionograms under the action of tidal winds (*black arrows*). The *blue arrows* indicate the presence of Es$_q$ trace. The *black vertical line* indicates the frequency where reflection from F layer starts (f_{min}F). In the ionograms, the overhead reflections for ordinary and extraordinary waves are *red* and *green*, respectively

frequency reflected from the F layer, f_{min}F, is listed in the right upper corner of each frame of Fig. 1. This minimum frequency increases from 3.62 MHz at 1415 UT to 3.7 MHz, at 1500 UT, after which it can be considered a blanketing Es layer (indicated by the red arrow). The f_{min}F reaches a maximum value of 3.93 MHz at 1545 UT after which it decreases until the Es$_b$ layer vanishes at 1615 UT.

The other analyzed event occurred on December 13, 2009 (dip = −5.35), a quiet day ($\sum$ Kp = 4, Dst > −2 nT), in which the Es$_b$ layer can be clearly observed in Fig. 2. This figure shows the ionograms between 1040 and 1550 UT; the Es$_b$ layer occurs from 1100 UT onwards, indicated by the red arrows. We named this as event W (Weaker EEJ event) in which the Es$_q$ traces can be seen in ionograms simultaneously with Es$_b$ layers, although they become less expressive than the Es$_b$ for this event.

The main difference between Es$_q$ and Es$_b$ is that the first is a diffuse trace in the ionogram that is transparent to radio signals, originated by instabilities in the EEJ. The Es$_b$ layers, on the other hand, can be formed by winds in low/midlatitudes, and they block the upper signal in ionograms. Only the frequencies higher than the blanketing frequency ($f > fb$Es) will propagate upwards and the reflected signal will be registered in the ionogram. When fbEs is higher than the F layer critical frequency (*fo*F2), no signal will be reflected from the F region. Indeed, most of the ionograms shown in S and W events belong

to the first category, i.e., the Es layer is partially blocking the upper layers in such a way that F layer can be observed at frequencies above fbEs. Although the condition fbEs > *fo*F2 is satisfied only in a few ionograms (see Fig. 2 at 1340 and 1400), it is clear the presence of Es$_b$ for both cases. In summary, in both cases the two types of Es, Es$_q$ and Es$_b$, are present, but in the first case the layer is under strong EEJ influence, while in the second this influence is weaker. Therefore, this allows us to investigate the role of the electric field in the formation or disruption of Es$_b$.

MIRE model and input parameters

The main purpose of this work is to simulate the competition between winds and electric fields in the Es$_b$ formation over Brazilian quasi-equatorial region. Thus, we used a specific model for simulating Es$_b$ layers, called MIRE [the Portuguese acronym for E Region Ionospheric Model (Carrasco et al. 2007)]. This theoretical model solves the continuity equation given by

$$\frac{\partial N_i}{\partial t} + \frac{\partial (V_{iz} N_i)}{\partial z} = P_i - L_i, \tag{1}$$

where N_i represents the number density of the ions, P_i and L_i represent the chemical production and loss, respectively, and V_{iz} is the vertical velocity of ions, which describes the vertical transport. Equation 1 is solved for

Resende *et al. Earth, Planets and Space* (2016) 68:201

Page 4 of 14
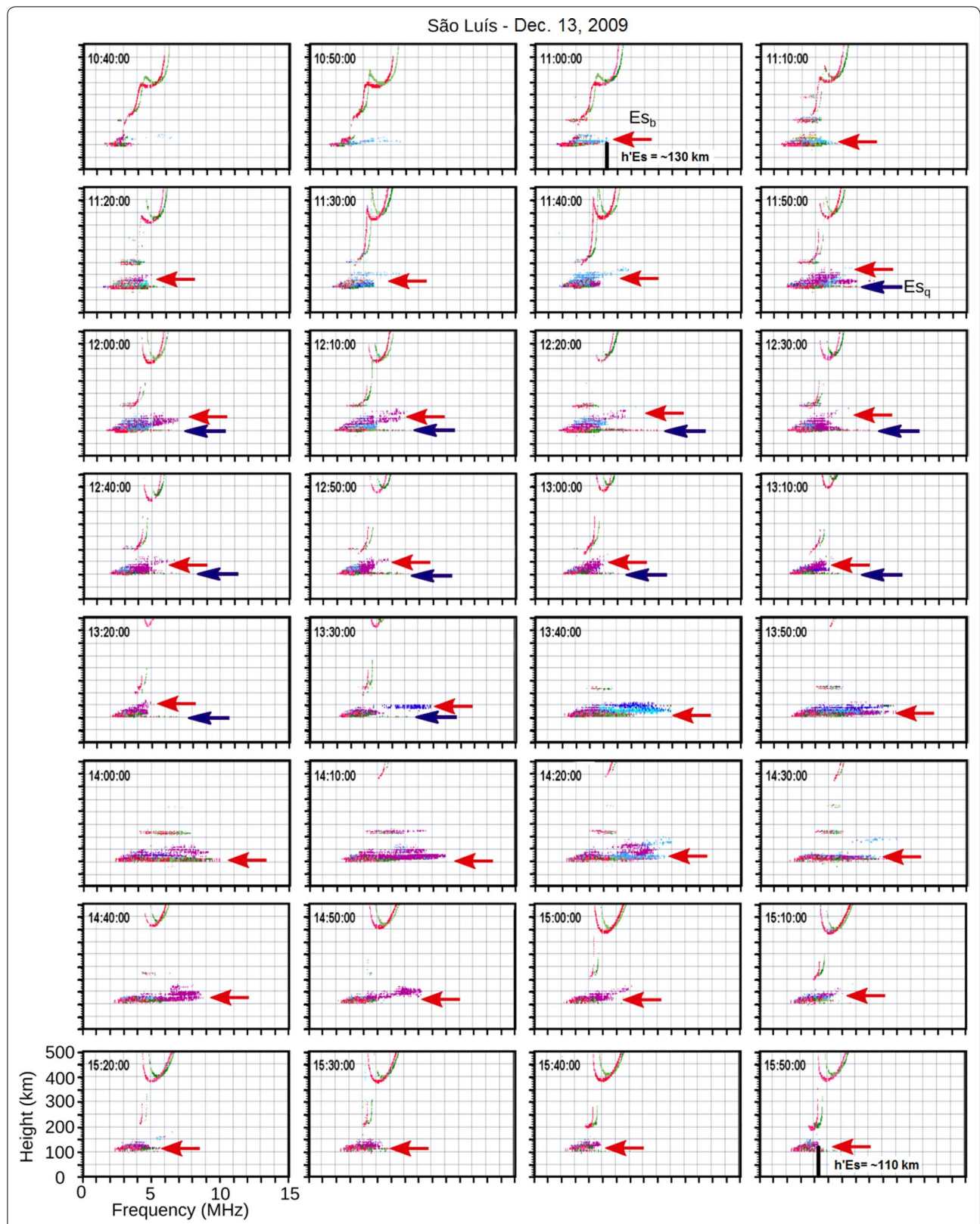
Fig. 2 Ionograms over São Luís on December 13, 2009, from 1040 to 1550 UT, *red arrows* indicate the presence of Es$_b$ layers. In the ionograms, the overhead reflections for ordinary and extraordinary waves are *red* and *green*, respectively. The *other colors* in the ionograms represent off-vertical reflections and are indicative of irregularities in the reflecting layer

Resende *et al. Earth, Planets and Space* (2016) 68:201

Page 5 of 14

the atomic oxygen ion (O^+), as well as of the main molecular (NO^+, O_2^+, N_2^+) and metallic (Fe^+, Mg^+) ions. The electron density, n_e, is obtained from the charge neutrality condition for the ionospheric plasma $n_e = \sum_i N_i$.

The chemical reactions as well as their coefficients are given in Carrasco et al. (2007). The vertical velocity, V_{iz}, as a function of electric fields and winds is given by

$$
\begin{aligned}
V_{iz} = \frac{\omega_i^2}{\left(\nu_{in}^2 + \omega_i^2\right)} & \left[\cos(I)\sin(I)U_x + \frac{\nu_{in}}{\omega_i}\cos(I)U_y \right. \\
& + \frac{1}{\nu_{in}}\frac{e}{m_i}\cos(I)\sin(I)E_x \\
& \left. + \frac{e}{\omega_i m_i}\cos(I)E_y + \frac{e}{\nu_{in}m_i}\left(\frac{\nu_{in}^2}{\omega_i^2} + \sin^2(I)\right)E_z \right],
\end{aligned}
\tag{2}
$$

where ω is the gyro frequency, I is the magnetic inclination, v is the collision frequency, e is the electron charge, m is the mass, U_y and U_x are the winds in eastward (zonal) and southward (meridional) directions, and E_x, E_y and E_z are the electric field components. The subscripts i and n refer to the ions and neutrals, respectively. Finite differences technique is applied to the differential equations (Eq. 1 for each ionic species), and the resulting set of discretized equations is solved using the Crank–Nicholson method (Press et al. 1985). The directions of the coordinate system are x (positive southward), y (positive eastward) and z (positive upward). The solution of the system of equations used in this model needs the atmospheric parameters such as the density of the atmospheric constituents, the temperature of the atmosphere, collision frequency and the height profile of the neutral iron density. All the input values to the model were explained in Carrasco et al. (2007). The system was solved using 0.05 km grid spacing in height between 86 and 140 km, and 2-min time step between 0000 and 2400 UT. At 0000 UT, the vertical profile of each species was calculated assuming photochemical equilibrium of the species and that profile was used as the initial condition. The numerical equations are solved iteratively until convergence was attained which generally happened after three complete 24-h cycles.

From Eq. 2, it is possible to see that the Es layer formation depends on the competition between tidal winds and electric fields. A vertical shear in V_{iz} is necessary for the formation of sporadic E layers which will be formed at the height where the velocity becomes null. The correct knowledge of the input parameters is a very important issue in the evaluation of their importance for the Es formation.

Therefore, the MIRE model includes the physics of Es layer development driven by tidal winds and electric fields. The neutral wind model that was considered here
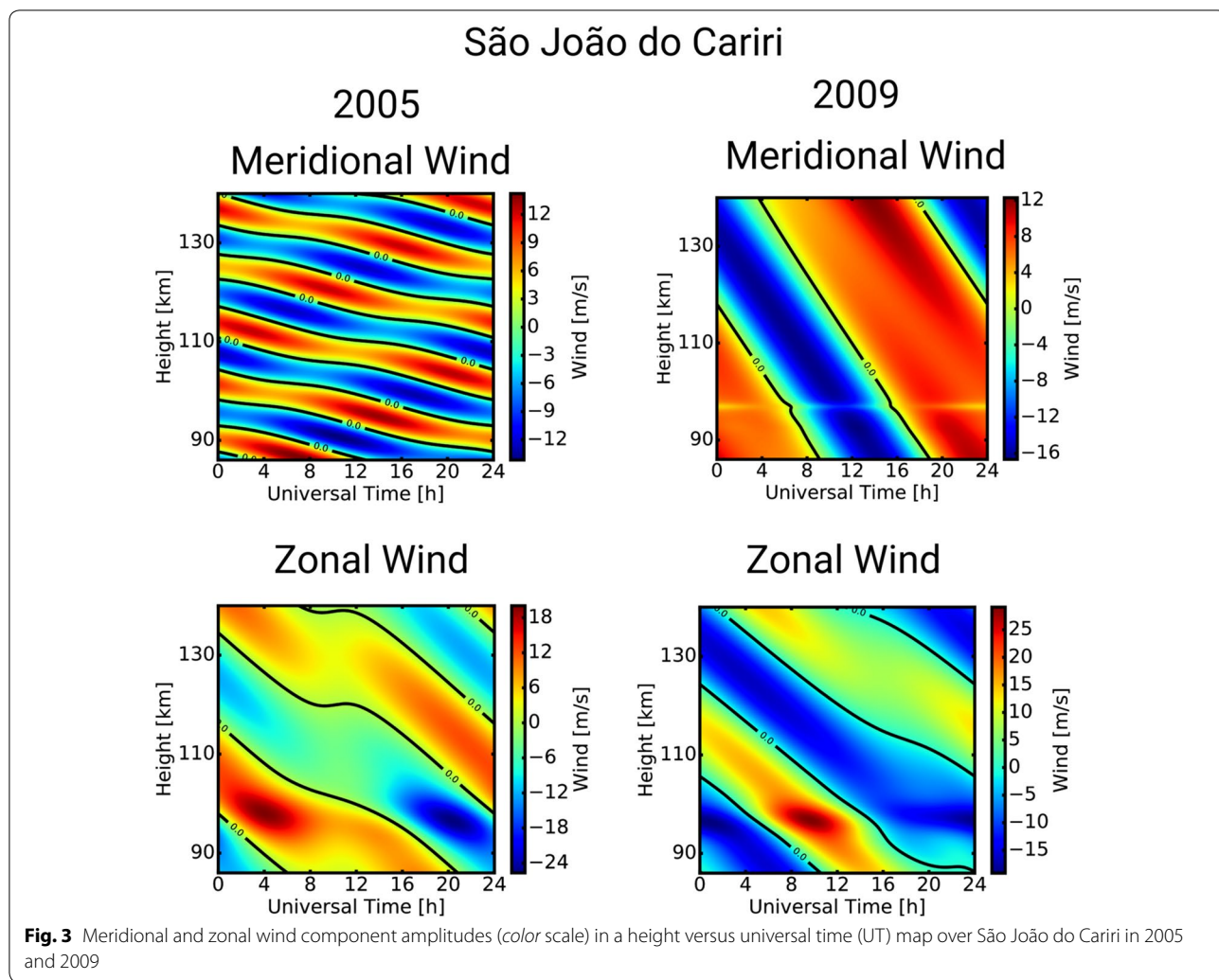
to simulate the Es_b layers over the Brazilian sector is outlined in Mathews and Bekeny (1979). The two horizontal wind components, U_y and U_x, can be written as

$$
U_y = U_{yo}\cos\left(\frac{2\pi}{\lambda}(z - z_o) + \frac{2\pi}{P}(t - t_o)\right),
\tag{3}
$$

$$
U_x = U_{xo}\sin\left(\frac{2\pi}{\lambda}(z - z_o) + \frac{2\pi}{P}(t - t_o)\right).
\tag{4}
$$

The parameter z_o represents a reference height supposed to be equal to 100 km, and P is the period of the tidal wind (24 h for diurnal and 12 h for semidiurnal tides). Such a wind model is characterized by the presence of nodal points ($U_x = 0$, $U_y = 0$) that allows the Es layer formation. However, the parameters used in Mathews and Bekeny (1979) were found incompatible over the Brazilian sector, providing misleading results compared to the observational data when used as input to MIRE. Therefore, in this study, we extend MIRE adding a novel neutral wind model derived from the all-sky meteor radar measurements, which provides more trustworthy results related to the Es layer formation in the Brazilian sector. For this novel wind model, the amplitude (U_{xo} and U_{yo}), phase (t_o) and vertical wavelength (λ) for the meridional and zonal components of the diurnal and semidiurnal tides were obtained from the observational winds derived from a meteor radar (SKiYMET) data in operation at São João do Cariri (SJC), Brazil (7° 4′ S, 36° 5′ W). The São João do Cariri data were used as a proxy for the equatorial region São Luís for which wind measurements are not available. The SKiYMET meteor radar is an all-sky interferometric radar that collects echoes from meteor ablation region. This radar allows resolutions of 1 h in time and 2 km in height for each day. The echoes are separated in height intervals for which the mean meridional and zonal winds are calculated. For each height interval, the meridional and zonal components of the diurnal and semidiurnal tides are fitted by the least mean square method and it is possible to find the components of the tide. Details about the methodology for inferring the tidal parameters are given in Andrioli et al. (2009).

Figure 3 shows the meridional and zonal wind components over SJC in a height versus universal time (UT) map format, in which we averaged the tidal parameters using the entire period of data, January, February and December for 2005 (a) and 2009 (b). It is possible to observe that the amplitudes (color scale) for both wind components are similar. The amplitudes of the meridional wind at SJC station do not exceed 16 m/s, being weaker than the amplitudes for the zonal wind (please, note that the scales of the figures are different). Furthermore, all the wind components exhibit shearing with respect to the

Resende *et al. Earth, Planets and Space* (2016) 68:201

Page 6 of 14

Fig. 3 Meridional and zonal wind component amplitudes (*color* scale) in a height versus universal time (UT) map over São João do Cariri in 2005 and 2009

height. However, there are some differences, such as the instant in which the wind shear occurs. In fact, Guharay et al. (2013) showed differences between the behavior of meridional and zonal wind components over São João do Cariri during 2005 and 2008. In their work, it is possible to note an enhancement in the semidiurnal tide in December 2008, which increases the confidence of the wind model used in our study. Additionally, the behavior of the neutral wind theoretical model presented here is in accordance with previous results in Buriti et al. (2008).

The observational data (tidal amplitudes, phases and vertical wavelength) are available for altitudes from 80 to 100 km. MIRE needs input parameters up to 140 km. Therefore, an extrapolation of the observational values was required. For the amplitudes, different fit curves were used for the diurnal and semidiurnal components, considering the theories about the wind behavior (Forbes and Garret 1979) at altitudes above 100 km. We used the

Lorentz curve for fitting the diurnal tide and the Gaussian fit for the semidiurnal tide. The phases of the tides were extrapolated by linear fitting to the observational data. The vertical wavelength is obtained by multiplying the linear coefficient of the fitted phase by the diurnal and semidiurnal tide periods, i.e., 24 and 12 h, respectively. Thus, we have a model constructed with experimental data from 80 to 100 km and extended up to 140 km based on the above described assumptions. It is important to mention that several fitting functions were tested for the tide amplitudes considering the theory about the wind behavior (Forbes and Garret 1979). It turns out that these Lorentz and Gaussian curves provided the best option for our data set. Also, our data indicate that the amplitudes of both diurnal and semidiurnal tides have a maximum below 100 km, decreasing for heights above that peak, supporting our decision for choosing such wind amplitude model. Finally, the temporal evolution of the tidal

Resende *et al. Earth, Planets and Space* (2016) 68:201

Page 7 of 14

winds, by using Eq. 3, was incorporated in MIRE model for the analyses of the Es$_b$ layers formation.

The zonal (E_y) and vertical (E_z) components of the electric field were inferred from measurements of the Doppler frequency of type II (gradient drift instability) echoes detected by the 50 MHz coherent back-scatter radar (RESCO) installed in São Luís with a height resolution of 2.6 km and 2-min time resolution (Abdu et al. 2002, 2003; Denardini et al. 2004, 2005, 2013, 2015). It is well known that Type II echoes are observed whenever the electron density gradient has a positive projection along E_z. Therefore, the Doppler frequency of type II echoes is proportional to E_z. The detailed methodology to infer the E_y and E_z components form RESCO data and the typical values of these components (0.5–1 mV/m for E_y component and 5–10 mV/m for E_z component) were recently reported by Moro et al. (2016a, b). The Doppler velocity of Type II irregularities (V_{DII}), in the EEJ, is associated with the drift velocity of E region electrons (V_e) according to the following equation:

$$V_{DII} = V_e \cdot (1 + \psi_o)^{-1}, \qquad (5)$$

where ψ_o is the anisotropic factor, which is the ratio of the electron to ion transverse mobility. The vertical component of the electric field (E_z) can be calculated through the relation $V_e = E_z \times B/B^2$, where V is positive westward is positive upward, and B is the geomagnetic field taken from the International Geomagnetic Reference Field (IGRF) model (Finlay et al. 2010) for São Luís region.

The E_y is deduced from E_z through the Hall (σ_2) to Pedersen (σ_1) geomagnetic field-line-integrated ionospheric conductivity ratio according to Eq. 6:

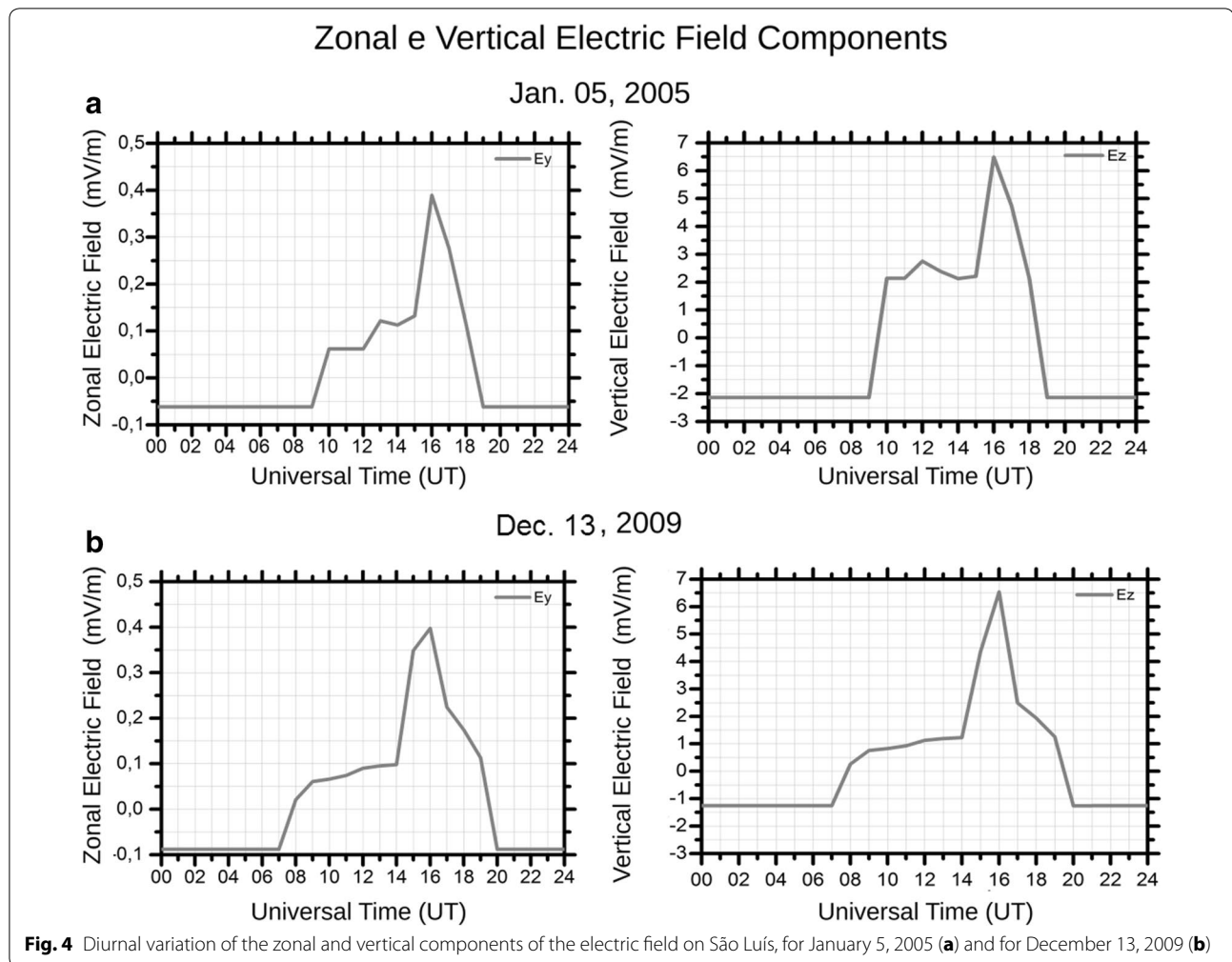$$E_z = \frac{\sum \sigma_2}{\sum \sigma_1} \times E_y. \qquad (6)$$

The Hall (σ_2) to Pedersen (σ_1) ionospheric conductivity is calculated using a model along the magnetic meridian overhead the RESCO radar site, and the field line coordinates with a grid resolution of 1 km. Also, the geomagnetic field-line-integrated ionospheric conductivity model is used to calculate the ionospheric conductivities. The ionospheric conductivity model has been recently updated to include several ionic and neutral species, with a new set of collision rate equations and the details are given in Moro et al. (2016a).

Figure 4 shows the zonal (left panel) and vertical (right panel) electric field components for January 5, 2005 and December 13, 2009. In these plots, we have considered the measurements at 105 km of altitude. In the absence of observational values for the nighttime period, we have used a constant value equal to the minimum observed during daytime, since the EEJ

current is not effective at nighttime. The electric field nighttime values are necessary because they are input parameters for the simulation. It is worthwhile noting the low values of the electric field components during the time period corresponding to the Es$_b$ layers occurrence in the ionograms. In general, the behavior of the electric fields in equatorial region reached the maximum of the 0.4 and 10 mV/m for the zonal and vertical component (Moro et al. 2016b), respectively, agreeing with the values of the electric field components in this work. However, the values reached the maximum from 10 UT (Moro et al. 2016a, b), and in our case the maximum occurs around 15–16 UT. In other words, we observed low values of electric fields in some hours for the diurnal period in the two specific cases. For January 2005, low values in the electric field components were observed until 15 UT, when they start to recover to typical values. On the ionograms for the same day (Fig. 1), the Es layer starts to appear at 1415 UT and an Es$_b$ layer becomes obvious at 1500 UT. The Es$_b$ layer lasts until 1530 UT agreeing with the low values of the electric fields, as seen in Fig. 4a. It is important to note that even though the E_z values are increasing between 1500 and 1530, the values are still low when compared to the typical ones (of the order of 5 to 10 mV/m). The E_z component reached around 3.5 mV/m in these hours. In relation to December 2009, the electric field components show low values until 14 UT when both components begin to grow and the vertical component reaches 6.5 mV/m at 16 UT. After that, both E_z and E_y decrease quickly. The Es$_b$ layers were observed from 1100 UT as seen in the ionograms of Fig. 2, and they were very strong until 1450 UT. After this, the Es$_b$ layer becomes weaker. Finally, the low values of electric field components cause the weakness of the EEJ current and the winds can be efficient and Es$_b$ layers are formed in equatorial regions. In order to try to simulate these effects on the Es layer formation through modeling, the E_z and E_y values shown in Fig. 4 were inserted in Eq. 2 in order to be used in MIRE model.

Results

The simulation was divided into different parts. Firstly, we run the model considering only the wind components influences, without introducing the electric field. Afterward, we have included the zonal and/or the vertical electric field components in order to evaluate their influence on the sporadic E formation or disruption process. Simulations considering only the effects of electric fields were also performed but are not shown here. The results for São Luís were as follows:

Resende *et al. Earth, Planets and Space* (2016) 68:201

Page 8 of 14

Fig. 4 Diurnal variation of the zonal and vertical components of the electric field on São Luís, for January 5, 2005 (**a**) and for December 13, 2009 (**b**)

## Results considering only the zonal and meridional wind components

Figure 5 shows the result of MIRE simulations on January 5, 2005 (part a) and on December 13, 2009 (part b) taking into account only the winds. In the figures, the electron density (in logarithm color code scale) is plotted as a function of time (in UT) and height. Es_b layers are clearly observed in both panels as descending layer along all day. On January 2005, the Es_b layer is formed above 130 km around 1600 UT and descends to approximately 98 km at 1100–1200 UT. For December 13, 2009, an Es_b layer is formed above 130 km around 0700 UT. This layer descends continuously even after 24 UT (note the continuity between the upper and lower layers from 2400 to 0000 UT) until it reaches approximately 98 km at around 2200 UT, when it is finally disrupted. Therefore, two layers were modeled between 0700 and 2200 UT. The descending movement of the Es layer, seen in the simulation results, is commonly observed in the ionograms as

well, and they are attributed to the semidiurnal or diurnal tidal winds (Haldoupis et al. 2006).

Results considering wind components and zonal component of the electric field (E_y)

The evolution of the E region electron density taking into account the zonal component of the electric field and tidal winds for January 5, 2005 is shown in Fig. 6a. In this case, the Es_b layer also appears during all day-long in our simulations similar to what is observed in Fig. 5a. Comparing this result with the previous one which considers only tidal winds (Fig. 5a), it is noted that electron density has smaller values during night-time and larger values during the day. Also, we observed that the phase transitions are different. In Fig. 5a (only winds), the phase transition occurred around 1500 UT, while in Fig. 6a the transitions occur at 0900 and 2100 UT. In this case, this layer descends continuously (even after 2400 UT) until it reaches approximately

Resende *et al. Earth, Planets and Space* (2016) 68:201

Page 9 of 14
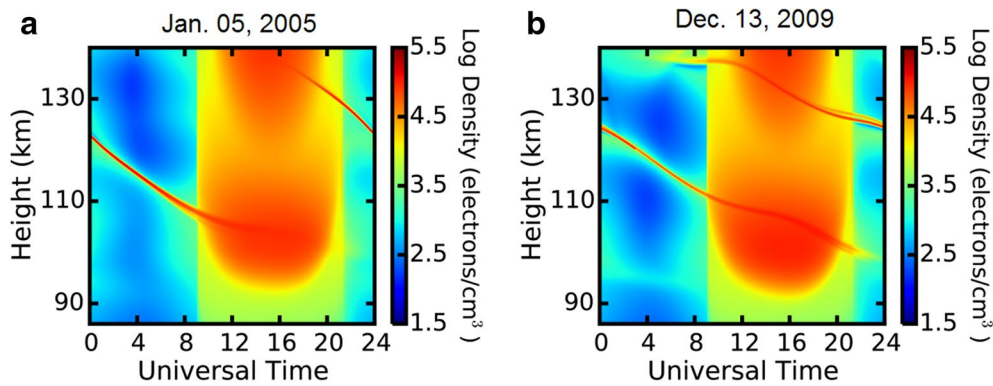
Fig. 5 Electron density as a function of time (UT) and altitude simulated by MIRE for January 5, 2005 (**a**) and for December 13, 2009 (**b**) considering only the tidal winds
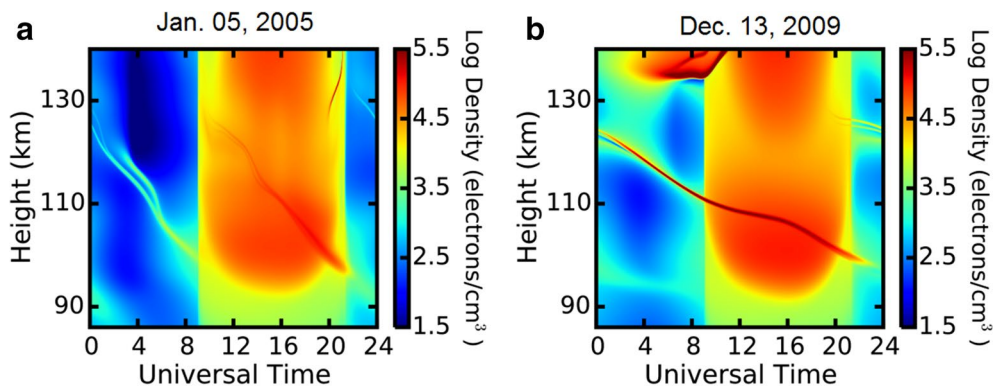
Fig. 6 Electron density as a function of time (UT) and altitude simulated by MIRE for January 5, 2005 (**a**), and for December 13, 2009 (**b**), considering the tidal winds and the zonal electric field component (E_y)
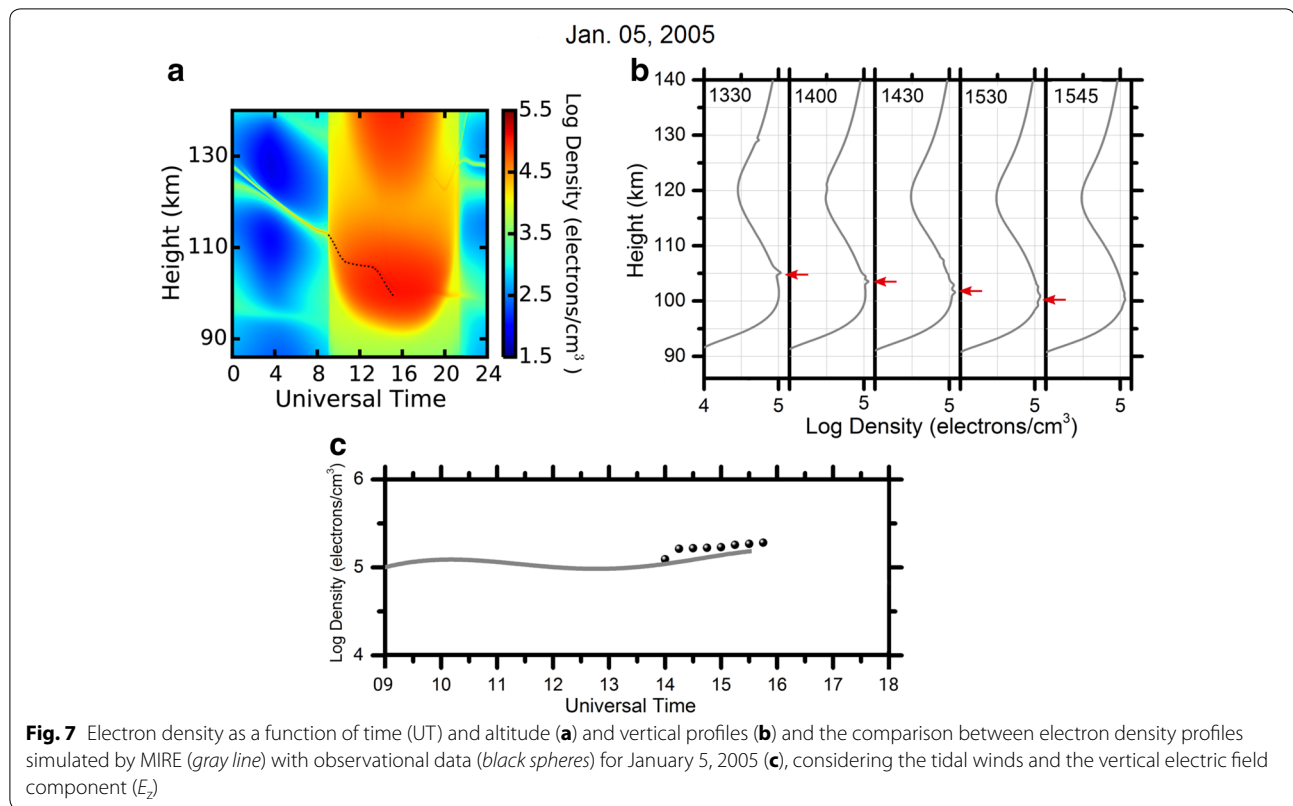
98 km at around 2200 UT, when it is finally disrupted. On December 13, 2009 (Fig. 6b), the upper layer starts to appear around 2000 UT, below 130 km. These results show that the addition of the zonal electric fields causes a modulation in the existing Es$_b$ layers which are still attributed to being developed by the tidal winds mechanism. This last statement comes from the fact that the electric fields are not efficient enough to create or disrupt any Es layers when suppressing the winds in our simulations (results not shown here).

Results considering wind components and the vertical component of the electric field (E_z)

Figure 7a, b present the Es$_b$ layer simulations considering winds and the vertical component of the electric field for the case study of January 5, 2005. Before 0900 UT and after 2100 UT, the simulated Es$_b$ layer exhibits low density values (between 103 and 104 electrons/cm^3). During daytime, the Es$_b$ layer occurs until 1530 UT, although its density is very close to the E region peak density, as can be seen in Fig. 7b (please note that the black dots in Fig. 7a were introduced in order to emphasize the Es$_b$ layers location and occurrence during this period, as the density was very close to the background E region density). The occurrence of the Es$_b$ layers is related to the lower values of the electric field components, and it agrees with the observations from ionograms for this day as can be seen in panel c of the same figure. In other words, the Es$_b$ layers can occur during the night because both components of the electric fields have low intensity. During daytime, it occurs only during the period in which E_z is low. In fact, during the period in which there are low values of the electric fields until 1530 UT (maximum E_z values around 3.5 mV/m), as seen in the RESCO radar data (Fig. 4, panel a), the Es$_b$ layer appears in the ionograms as well as in the simulation using MIRE.

Simulations for December 13, 2009, are shown in Fig. 8a, in which the black dots were again introduced to

Resende *et al. Earth, Planets and Space* (2016) 68:201

Page 10 of 14

Fig. 7 Electron density as a function of time (UT) and altitude (**a**) and vertical profiles (**b**) and the comparison between electron density profiles simulated by MIRE (*gray line*) with observational data (*black spheres*) for January 5, 2005 (**c**), considering the tidal winds and the vertical electric field component (E_z)

emphasize the Es_b layers location and occurrence. This was the W event for which the intensity of the vertical component of the electric field was lower (Fig. 4, panel b). The simulation results show that the Es_b layer density is higher when compared to the Es_b layer simulations in 2005 (see Figs. 7b, 8b). The Es_b layers appear during the nighttime, and they last until 1445 UT. During this year, the EEJ current was considered weak due to the displacement of the magnetic equator away from São Luís. Therefore, the Es_b traces in ionograms are stronger than the irregularity traces, Es_q, most of the time (see Fig. 2). In both cases, the results show that high values of electric fields can overcome the effect of the tidal winds in such a way that Es_b layers are not observed. However, when the electric field intensity decreases, the tidal wind effect can become dominant and the Es_b layers can occur.

Results considering the wind components and the zonal (E_y) and vertical (E_z) components of the electric field components

These results are very similar to those shown in Figs. 7 and 8 found when considering only the vertical electric field component. This means that the vertical component of the electric field is determinant for the Es_b layer occurrence, in such a way that Es_b layer only occurs under low E_z values.

Discussion and conclusions

In this paper, we have analyzed the effect of the electric fields on the formation of blanketing sporadic E layers over São Luís, a transition region very close to the magnetic equator. São Luís is an interesting region because this station lies in a transition region, since the geomagnetic equator is being driven away due to the secular variation of the Earth's magnetic field. This drift, in turn, provides an apparent northwestward movement of the geomagnetic equator at a rate of ~9′/year (~16 km/year). In this region, we can observe two different types of Es layers: a diffuse, Es_q; and the Es_b layers formed by wind shear. Therefore, this competition was simulated using an E region model, MIRE, for which the input parameters, winds and electric fields, for the equatorial region were included. The analysis was performed for two different situations under strong EEJ influence on January 5, 2005, and under weaker EEJ influence on December 13, 2009.

The initial simulation considered only the tidal winds components (meridional and zonal). The Es_b layers appear during all day for both the dates analyzed. Moreover, on December 13, 2009, two layers were seen simultaneously in the profile. It is observed that the Es_b layers are seen in both cases. Moreover, these Es_b layers have a downward movement, which agrees with the accepted theory of the Es_b layers due to tidal winds (Bishop and

Resende *et al. Earth, Planets and Space* (2016) 68:201

Page 11 of 14

Fig. 8 Electron density as a function of time (UT) and altitude (**a**) and vertical profiles (**b**) simulated by MIRE considering the tidal winds and the vertical electric field component (E_z) and electron density model using tidal winds (*gray line*) together with the observational data (**c**) for December 13, 2009
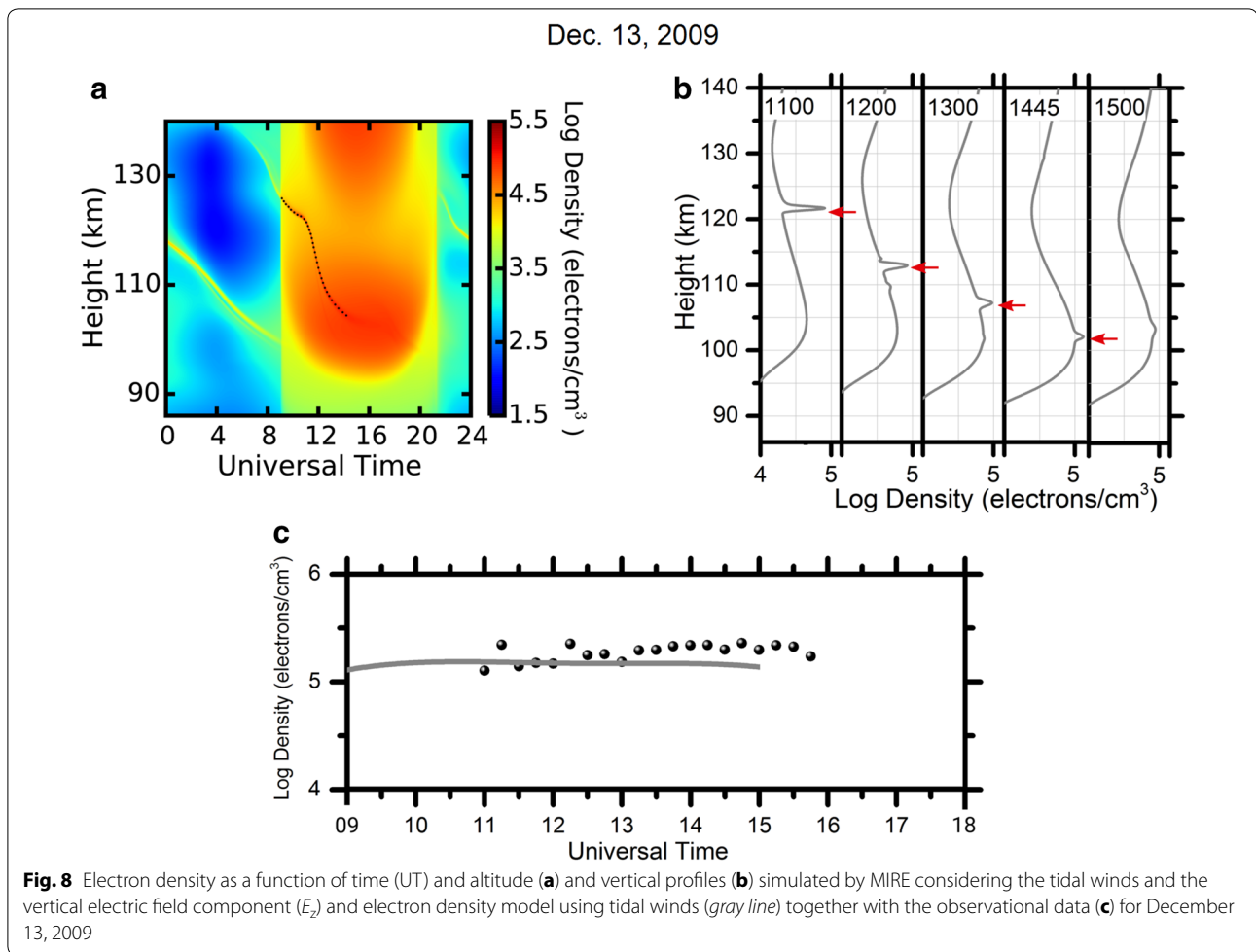
Earle 2003; Haldoupis 2011). Therefore, our results support that the tidal wind measurements used as input model are effectively capable of forming Es_b layers in São Luís, even though the wind data were obtained from São João do Cariri station.

In relation to electric fields, we used the vertical and zonal components obtained from Doppler frequency of type II echoes measured by the RESCO radar. During the observations of the Es_b layers in the ionograms, it is noted that the electric field components intensity decrease in both days. In our simulations, electric fields alone are not able to generate Es_b layers. In other words, the Es_b layers were produced by the winds but the EEJ electric field can have some effect (increase/disruption) on these layers. This fact is known and reported by other authors (Rastogi 1971; Reddy and Devasia 1973; Rastogi 1997).

In this study, when we have considered the E_y, there were few changes in Es_b layers comparing to the results when only tidal winds were considered. This simulation has shown that the zonal component of the electric field has a significant effect on the phase of the descending Es layers.

These results were similar to those presented by Dagar et al. (1977), in which similar electric fields values were used for an equatorial station. The Es_b layers have shown an increase in frequency when considering the zonal component of the electric field and tidal winds together. However, Dagar et al. (1977) concluded that the values of the zonal component of the electric fields, even with winds influence, could form Es_b layers when their values were smaller than 2 mV/m. In our study, the values of the electric fields zonal component do not exceed 0.5 mV/m and the MIRE can simulate the Es_b layers over the whole day with these values. Furthermore, Dagar et al. (1977) estimated similar values of the zonal electric field to analyze any influence in the Es layer. They found that this electric field component increases the Es layer electron density. However, no analysis regarding the Es layer phase was provided.

Abdu et al. (2003) showed that a negative gradient of the ion velocity (dV_{iz}/dt) is necessary to produce the convergence of the electron density in such way that a sporadic E layer may be formed in the low-latitude ionosphere. Also, they stated that such negative gradient does

Resende *et al. Earth, Planets and Space* (2016) 68:201

Page 12 of 14

not exclude the need for a wind shear in the wind components. In this case, the Es layer can also be formed by a steady, height-independent, westward zonal wind that produces a negative vertical gradient in the vertical ion velocity, which, in turn, leads to ionization convergence. Therefore, a possibility is that the Es layer in MIRE model can be caused by this former mechanism in addition to wind shear. The zonal electric field component included in the vertical ion velocity (Eq. 1) can cause this behavior of the Es_b layer in the MIRE simulations.

The vertical component of electric field is higher than the zonal component, and it is the most important for the EEJ development (Forbes 1981). The Es_b layers occur when the vertical component of the electric field has a decrease in its values. During the Event S, the Es_b layers appear during nighttime when E_z is small. In fact, the zonal electric field during the night is reversed (west direction), the gradient drift irregularities are weak and the winds can play a role in the formation of Es layers (Whitehead 1961, Rastogi 1971). Furthermore, the Es_b layers also occur at daytime during some specific hours when the vertical component is low. In these cases, the peak density is very close to the E region background density. On the other hand, the Es_b layers on Event W appear with a greater intensity in our simulations, because of the lower E_z values during most of the day. This agrees well with the observations seen in the ionograms, which show stronger Es_b in 2009 (Fig. 2) than in 2005 (Fig. 1). In fact, the vertical component of the electric field is considered the main factor for Es_b layers formation in the equatorial region. In our simulations, a threshold value for the vertical electric field component equal to 3.85 mV/m was found. In other words, MIRE model was not capable of simulating Es_b layers when E_z values exceed this threshold. When the zonal and vertical electric field components are considered together, the simulation results were very similar to those considering only the vertical component, which reinforces the importance of E_z component on the Es_b occurrence.

The electric fields present in the equatorial E region can generate plasma irregularities that are seen in ionograms as Es_q traces and, at the same time, can inhibit the Es_b layers formation. This last point (the inhibition of Es_b layer by electric fields) is evident in the results from the simulation for São Luís. Reddy and Devasia (1973) studied the electric field in the equatorial region, and they showed that Es_b layers in ionograms do not occur during the day, since the irregularities are stronger and the electric field inhibits the Es_b formation. Devasia et al. (2004, 2006) analyzed the Es_b layers at specific hours over equatorial regions, and they connected these layers with Counter Electrojet events (CEJ), when the EEJ current

was reversed. During this inversion, the vertical component of the electric field is weak or with the opposite direction and, thus, Es_b layers were formed. In our study, the CEJ did not occur, but the electric field vertical component intensity decreased in relation to its typical value [approximately around 5 to 10 mV/m (Denardini et al. 2013)]. The hypothesis for Event S could be some perturbation present in the ionosphere during this period, but we do not have enough information to confirm this. In Event W, the low values of E_z confirm that the position of São Luís station in relation to the magnetic equator has changed (dip angle has increased) in relation to the year 2005 and, for this reason, Es_b layers are more frequently observed in this year.

Carrasco et al. (2007) analyzed the vertical electric field influence in the Es layers during the F region pre-reversal enhancement (PRE) in the zonal electric fields, through the mapping of these electric fields through the equipotential magnetic field lines. However, the main purpose of Carrasco et al. (2007) was to observe the disruption or enhancement of the Es layer around sunset and its correlation with the PRE, depending of the direction of the vertical electric field component. Also, Abdu et al. (2014) investigated of low-latitude Es layers during magnetic storms and concluded that the formation and disruption of these layers are strongly controlled by the magnetospheric electric fields. However, in our work the main purpose is to quantify the role of winds and electric fields in the Es layer formation over a peculiar equatorial region. Thus, this study is concentrated during the diurnal period since the EEJ is effective in these hours. The Es_b and Es_q layer observations are very similar to what was observed by Abdu et al. (1996) over Fortaleza, also in the Brazilian region. They found that the Es_q layers occurrence decreased systematically as the magnetic equator moved away from this region as it occurs in São Luís. In our analysis, São Luís was still under the magnetic equator influence in 2005 and 2009, and thus two mechanisms can compete, neutral winds and electric fields, which are the responsible for the Es_b layers formation or disruption. The secular variation on the geomagnetic field and its effect on the EEJ over Brazil is investigated by Moro et al. (2016c).

In fact, in our simulations, MIRE shows Es_b layers only in specific hours when vertical component of the electric field is low. In other words, the presence of Es_b layer means that the wind shear mechanism is dominant. We believe that the vertical electric field component is responsible for the Type II irregularities in the E region plasma of the equatorial station. This irregularity will be generated under normal EEJ conditions only when both the vertical polarization electric field and the vertical electron density gradient are parallel and they can be observed by the VHF backscatter radars by the strong

Resende *et al. Earth, Planets and Space* (2016) 68:201

Page 13 of 14

scattered echoes (Devasia et al. 2006). Therefore, when the vertical polarization electric field is low, the irregularities are weak also. This behavior is observed in our cases studied, in which there is a weakness/disruption of the Es_q layers in ionograms and simulations. In conclusion, as the magnetic equator moves away from São Luís, the vertical electric field responsible by Type II irregularity formation becomes weak and the tidal winds are more effective during these hours. Therefore, the vertical component of the electric field is the main agent responsible for the Es_b layer disruption.

Another characteristic is that the Es_b layers simulated with MIRE model reveal a typical downward movement pattern when we included the electric fields in our simulations also. In Fig. 6 (E_y + winds) and Figs. 7 and 8 (E_z + winds), the descending pattern is very clear in all cases. In general, the Es_b layers are formed at high altitudes (above 130 km) and descend to below 100 km. This behavior was also observed on the ionograms in midlatitudes (Bishop and Earcle 2003; Haldoupis et al. 2006). The movement occurs due to the semidiurnal and diurnal tide winds that are responsible for the Es layers formation. In summary, the downward propagating wind shear nodes transport the ion layers formed at the nodes to lower altitudes (Chimonas and Axford 1968).

Finally, in this study we were able to simulate Es_b layers occurrence using realistic values for electric fields from observational data and tide wind profile based on observational data from 80 to 100 km. Electric fields and winds from observations were included in MIRE model in order to verify the Es_b formation. The results are in good agreement with observations from ionograms and with other theoretical studies about the Es_b occurrence. Furthermore, with this simulation it was possible to show the importance of the tidal wind profile on the sporadic E layers and also that the electric field induced from the equatorial electrojet can inhibit the wind effect close to equatorial regions. In our study, a vertical electric field higher than 3.85 mV/m (threshold value) will disrupt the Es_b layers.

Authors' contributions
LCAR, ISB, CMD, VFA and PPB designed the study, analyzed and interpreted the data and wrote the manuscript. JM and SSC helped to improve the manuscript. All authors read and approved the manuscript.

Author details
[1] National Institute for Space Research (INPE), São José dos Campos, SP, Brazil. [2] Physics Department, Universidad de Los Andes, Mérida, Venezuela. [3] National Space Science Center, Chinese Academy of Science, Beijing, China. [4] Southern Regional Space Research Center (CRS/INPE), Santa Maria, RS, Brazil.

References
Abdu MA, Batista IS, Muralikrishna P, Sobral JHA (1996) Long-term trends in sporadic E layers and electric fields over Fortaleza. Braz Geophys Res Lett 23(7):757–760. doi:10.1029/96GL00589

Abdu MA, Denardini CM, Sobral JHA, Batista IS, Muralikrishna P, De Paula ER (2002) Equatorial Electrojet Irregularities Investigations Using a 50 MHz Back-Scatter Radar and a Digisonde at São Luís: some Initial Results. J Atmos Solar-Terr Phys 64(12):1425–1434. doi:10.1016/j.jastp.2003.08.011

Abdu MA, Denardini CM, Sobral JHA, Batista IS, Muralikrishna P, Iyer KN, Véliz Ó, De Paula ER (2003) Equatorial electrojet 3-m irregularity dynamics during magnetic disturbances over Brazil: results from the New VHF radar at São Luís. J Atmos Solar-Terr Phys 65(14):1293–1308. doi:10.1016/S1364-6826(02)00106-2

Abdu MA, Souza JR, Batista IS, Santos AM, Sobral JHA, Rastogi RG, Chandra H (2014) The role of electric fields in sporadic E layer formation over low latitudes under quiet and magnetic storm conditions. J Atmos Solar-Terr Phys 115:95–105. doi:10.1016/j.jastp.2013.12.003

Andrioli VF, Clemesha BR, Batista PP, Schuch JN (2009) Atmospheric tides and mean winds in the meteor region over Santa Maria (29.7S;53.8 W). J Atmos Solar-Terr Phys 71(17):1864–1876. doi:10.1016/j.jastp.2009.07.005

Axford WI (1963) The formation and vertical movement of dense ionized layers in the ionosphere due to neutral wind shears. J Geophys Res 68(3):769–779. doi:10.1029/JZ068i003p00769

Batista IS, Diogo EM, Souza JR, Abdu MA, Bailey GJ (2011) Equatorial ionization anomaly: the role of thermospheric winds and the effects of the geomagnetic field secular variation. Aeronomy of the earth's atmosphere and ionosphere, 1edn. Springer, 2:317–328. doi:10.1007/978-94-007-0326-1_23

Bishop RL, Earle GD (2003) Metallic ion transport associated with midlatitude intermediate layer development. J Geophys Res 108(A1):10–19. doi:10.1029/2002JA009411

Buriti RA, Hocking WK, Batista PP, Medeiros AF (2008) Observations of equatorial mesospheric winds over Cariri (7.4° S) by a meteor radar and comparison with existing models. Ann Geophys 26:485–497. doi:10.5194/angeo-26-485-2008

Carrasco AJ, Batista IS, Abdu MA (2007) Simulation of the sporadic E layer response to pre-reversal associated evening vertical electric field enhancement near dip equator. J Geophys Res 112(A06):324–335. doi:10.1029/2006JA012143

Chandra H, Rastogi R (1975) Blanketing sporadic E layer near the magnetic equator. J Geophys Res 80(1):149–153. doi:10.1029/JA080i001p00149

Chimonas G, Axford WI (1968) Vertical movement of temperate zone sporadic E layers. J Geophys Res 73(1):111–117. doi:10.1029/JA073i001p0011

Dagar R, Verma P, Napgal O, Setty CSGK (1977) The relative effects of the electric fields and neutral winds on the formation of the equatorial sporadic layers. Ann Geophys 33(3):333–340

Denardini CM, Abdu MA, Sobral JHA (2004) VHF radar studies of the equatorial electrojet 3-m irregularities over São Luís: day-to-day variabilities under auroral activity and quiet conditions. J Atmos Solar-Terr Phys 66(17):1603–1613. doi:10.1016/j.jastp.2004.07.031

Denardini CM, Abdu MA, De Paula ER, Sobral JHA, Wrasse CM (2005) Seasonal characterization of the equatorial electrojet height rise over Brazil as observed by the RESCO 50 MHz back-scatter radar. J Atmos Solar-Terr Phys 67:1665–1673. doi:10.1016/j.jastp.2005.04.008

Denardini CM, Aveiro HC, Sobral JHA, Bageston JV, Guizelli LM, Resende LCA, Moro J (2013) E region electric fields at the dip equator and anomalous

Resende *et al. Earth, Planets and Space* (2016) 68:201

Page 14 of 14

conductivity effects. Adv Space Res 51(10):1857–1869. doi:10.1016/j.asr.2012.06.003

Denardini CM, Moro J, Resende LCA, Chen SS, Schuch NJ, Costa JER (2015) E region electric field dependence of the solar activity. J Geophys Res Space Phys 120:8934–8941. doi:10.1002/2015JA021714

Devasia CV, Jyoti N, Subbarao KSV, Tiwari D, Raghava RC, Sridharan R (2004) On the role of vertical electron density gradients in the generation of type II irregularities associated with blanketing Es (Es$_b$) during counter equatorial electrojet events: a case study. Radio Sci 39(RS3007):1–14. doi:10.1029/2002RS002725

Devasia CV, Sreeja V, Ravindran S (2006) Solar cycle dependent characteristics of the equatorial blanketing Es layers and associated irregularities. Ann Geophys 24(11):2931–2947. doi:10.5194/angeo-24-2931-2006

Fambitakoye O, Rastogi RG, Tabbagh J, Vila P (1973) Counter electrojet and Esq disappearance. J Atmos Solar-Terr Phys 35:119–1126. doi:10.1016/0021-9169(73)90009-3

Finlay CC, Maus S, Beggan CD, Bondar TN, Chambodut A, Chernova TA, Chulliat A, Golovkov VP, Hamilton B, Hamoudi M, Holme R, Hulot G, Kuang W, Langlais B, Lesur V, Lowes FJ, Lühr H, Macmillan S, Mandea M, Mclean S, Manoj C, Menvielle M, Michaelis I, Olsen N, Rauberg J, Rother M, Sabaka TJ, Tangborn A, Tøffner-Clausen L, Thébault E, Thomson AWP, Wardinski I, Wei Z, Zvereva TI (2010) International geomagnetic reference field: the eleventh generation. Geophys J Int 183:1216–1230

Forbes JM (1981) The equatorial electrojet. Rev Geophys 19(3):469–504. doi:10.1029/RG019i003p00469

Forbes JM, Garret HB (1979) Theoretical studies of atmospheric tides. Rev Geophys 17(8):1951–1981. doi:10.1029/RG017i008p01951

Guharay A, Batista PP, Clemesha BR, Sarkhel S (2013) On the variability of the terdiurnal tide over a Brazilian equatorial station using meteor radar observations. J Atmos Sol Terr Phys 104:87–95. doi:10.1016/j.jastp.2013.08.021

Haldoupis C (2011) A tutorial review on sporadic E layers, aeronomy of the earth's atmosphere–ionosphere. IAGA book series. 29:381–394. doi:10.1007/978-94-007-0326-1_29

Haldoupis C, Meek C, Christakis N, Pancheva D, Bourdillon A (2006) Ionogram height-time intensity observations of descending sporadic E layers at mid-latitude. J Atmos Solar-Terr Phys 68(539):539–557. doi:10.1016/j.jastp.2005.03.020

Haldoupis C, Pancheva D, Singer W, Meek C, Mac-Dougall J (2007) An explanation for the seasonal dependence of midlatitude sporadic E layers. J Geophys Res 112:A06315. doi:10.1029/2007JA012322

Knecht RW, McDuffie RE (1962) On the width of the equatorial Es belt. In: Smith EK, Matsushita S (eds) Ionospheric sporadic E. Pergamon Press, New York, p 215

Kopp E (1997) On the abundance of metal ions in the lower ionosphere. J Geophys Res 102:9667–9674. doi:10.1029/97JA00384

Layzer D (1972) Theory of midlatitude sporadic E. Radio Sci 7(3):385–395. doi:10.1029/RS007i003p00385

Mathews JD (1998) Sporadic E: current views and recent progress. J Atmos Solar-Terr Phys 60(4):19–58. doi:10.1016/S1364-6826(97)00043-6

Mathews JD, Bekeny FS (1979) Upper atmosphere tides and the vertical motion of ionospheric sporadic layers at Arecibo. J Geophys Res 84(A6):2743–2750. doi:10.1029/JA084iA06p02743

Moro J, Denardini CM, Resende LCA, Chen SS, Schuch NJ (2016a) Influence of uncertainties of the empirical models for inferring the E-region electric fields at the dip equator. Earth Planets Space 68:103. doi:10.1186/s40623-016-0479-0

Moro J, Denardini CM, Resende LCA, Chen SS, Schuch NJ (2016b) Equatorial E-region electric fields at the dip equator—I. Variabilities in eastern Brazil and Peru. J Geophys Res Space Phys 121:10220–10230. doi:10.1002/2016JA022751

Moro J, Denardini CM, Resende LCA, Chen SS, Schuch NJ (2016c) Equatorial E-region electric fields at the dip equator—II. Seasonal variabilities and effects over Brazil due to the secular variation of the magnetic equator. J Geophys Res Space Phys 121:10231–10240. doi:10.1002/2016JA022753

Oikonomou C, Haralambous H, Haldoupis C, Meek C (2014) Sporadic E tidal variabilities and characteristics observed with the Cyprus Digisonde. J Atmos Solar-Terr Phys 119:173–183. doi:10.1016/j.jastp.2014.07.014

Piggot W, Rawer K (1972) Handbook of ionogram interpretation and reduction, Edited by US Department of Commerce, p 352

Pignalberi A, Pezzopane M, Zuccheretti E (2014) Sporadic E layer at midlatitudes: average properties and influence of atmospheric tides. Ann Geophys 32:1427–1440. www.ann-geophys.net/32/1427/2014/

Press WH, Teukolsky S, Vetterling WT, Flannery BP (1985) Numerical recipes. Cambridge University Press, Cambridge

Rastogi RG (1971) Equatorial sporadic E and cross-field instability. Ann Geophys 28(4):717–727

Rastogi RG (1997) Midday reversal of equatorial ionospheric electric field. Ann Geophys 15:1309–1315. doi:10.1007/s00585-997-1309-2

Reddy CA, Devasia CV (1973) Formation of blanketing sporadic E layers at the magnetic equator due to horizontal wind shears. Planet Space Sci 21(5):811–817. doi:10.1016/0032-0633(73)90098-6

Resende LCA, Denardini CM, Batista IS (2013) Abnormal fbEs enhancements in equatorial Es layers during magnetic storms of solar cycle 23. J Atmos Solar-Terr Phys 102:228–234. doi:10.1016/j.jastp.2013.05.020

Tsunoda RT (2008) On blanketing sporadic E and polarization effects near the equatorial electrojet. J Geophys Res 113:A09304. doi:10.1029/2008JA01315

Whitehead J (1961) The formation of the sporadic-E in the temperate zones. J Atmos Solar-Terr Phys 20(1):1155–1167. doi:10.1016/0021-9169(61)90097-6

Wilkinson PJ, Szuszczewicz EP, Roble RG (1992) Measurements and modelling of intermediate, descending, and sporadic layers in the lower ionosphere: results and implications for global-scale ionospheric-thermospheric studies. Geophys Res Lett 19(2):95–98. doi:10.1029/91GL02774

Yadav V, Kakad B, Nayak CK, Surve G, Emperumel K (2014) Occurrence of blanketing Es layer (Es$_b$) over the equatorial region during the peculiar minimum of solar cycle 24. Ann Geophys 32:553–562. doi:10.5194/angeo-32-553-2014